HAL
open science

Future sensitivity to new physics in B_d, B_s and K mixings

Jérôme Charles, Sebastien Descotes-Genon, Zoltan Ligeti, Stephane Monteil, Michele Papucci, Karim Trabelsi

To cite this version:

Jérôme Charles, Sebastien Descotes-Genon, Zoltan Ligeti, Stephane Monteil, Michele Papucci, et al.. Future sensitivity to new physics in B_d, B_s and K mixings. Physical Review D, 2014, 89, pp.033016. 10.1103/PhysRevD.89.033016 . hal-00862357

HAL Id: hal-00862357
https://hal.science/hal-00862357v1

Submitted on 23 Nov 2023

HAL is a multi-disciplinary open access archive for the deposit and dissemination of scientific research documents, whether they are published or not. The documents may come from teaching and research institutions in France or abroad, or from public or private research centers.

L'archive ouverte pluridisciplinaire **HAL**, est destinée au dépôt et à la diffusion de documents scientifiques de niveau recherche, publiés ou non, émanant des établissements d'enseignement et de recherche français ou étrangers, des laboratoires publics ou privés.

Future sensitivity to new physics in B_d, B_s and K mixings

Jérôme Charles*,[1,2] Sébastien Descotes-Genon*,[3] Zoltan Ligeti,[4]
Stéphane Monteil*,[5] Michele Papucci,[6] and Karim Trabelsi*[7]

[1] *Aix-Marseille Université, CNRS, CPT, UMR 7332, 13288 Marseille, France*
[2] *Université de Toulon, CNRS, CPT, UMR 7332, 83957 La Garde, France*
[3] *Laboratoire de Physique Théorique, CNRS/Univ. Paris-Sud 11 (UMR 8627) 91405 Orsay Cedex, France*
[4] *Ernest Orlando Lawrence Berkeley National Laboratory, University of California, Berkeley, CA 94720*
[5] *Laboratoire de Physique Corpusculaire de Clermont-Ferrand Université Blaise Pascal 24 Avenue des Landais F-63177 Aubiere Cedex*
[6] *Michigan Center for Theoretical Physics, University of Michigan, Ann Arbor, MI 48109*
[7] *High Energy Accelerator Research Organization, KEK 1-1 Oho, Tsukuba, Ibaraki 305-0801, Japan*
**for the CKMfitter Group*

arXiv:1309.2293v3 [hep-ph] 27 Feb 2014

We estimate, in a large class of scenarios, the sensitivity to new physics in B_d and B_s mixings achievable with $50\,\mathrm{ab}^{-1}$ of Belle II and $50\,\mathrm{fb}^{-1}$ of LHCb data. We find that current limits on new physics contributions in both $B_{d,s}$ systems can be improved by a factor of ~ 5 for all values of the CP violating phases, corresponding to over a factor of 2 increase in the scale of new physics probed. Assuming the same suppressions by CKM matrix elements as those of the standard model box diagrams, the scale probed will be about 20 TeV for tree-level new physics contributions, and about 2 TeV for new physics arising at one loop. We also explore the future sensitivity to new physics in K mixing. Implications for generic new physics and for various specific scenarios, such as minimal flavor violation, light third-generation dominated flavor violation, or $U(2)$ flavor models are studied.

I. INTRODUCTION

Before the impressive results from the B factory experiments, BaBar and Belle, the simple picture of Kobayashi and Maskawa for the origin of the CP violation [1] observed in K decays was not confirmed experimentally. The BaBar and Belle results showed that the SM description of the flavor sector is correct at the order one level. However, in most flavor-changing neutral-current processes, new physics (NP) can still contribute at least at the level of 20–30% compared to the SM.

Many extensions of the SM receive stringent constraints from data on flavor changing processes and CP violation, and may give observable effects as the sensitivity improves. The mixings of the four neutral mesons, K, D, B_d, and B_s, provide particularly strong bounds. For each neutral-meson system, contributions generated by new heavy degrees of freedom can be described by two real parameters. For example, in low-energy supersymmetry B mixing receives contributions (besides the SM box diagrams with W bosons and top quarks) from box diagrams with winos and stops or gluinos and sbottoms. The magnitudes and phases of such contributions depend crucially on the mechanism of supersymmetry breaking and the origin of flavor symmetry breaking.

However, the extraction of NP contribution to meson mixing is entangled with the determination of the SM parameters, in particular the CKM elements. It is not enough to measure the mixing amplitude itself, only the combination of many measurements can reveal a deviation from the SM. In this paper we perform such a fit, taking into account the latest expectations for future LHCb and Belle II measurements, and anticipated progress in lattice QCD, in order to investigate the sensitivity to NP in neutral-meson mixing in the near future.

In most of this paper, we consider the well-defined scenario where no deviations from the SM predictions are observed. This allows us to explore the expected progress in constraining NP in the mixings of neutral mesons in an unambiguous way. An illustration of the prospects to reveal a possible NP signal is given in the last section.

II. NEW PHYSICS IN MESON MIXING

In a large class of NP models the unitarity of the CKM matrix is maintained, and the most significant NP effects occur in observables that vanish at tree level in the SM. In the SM CKM fit, the constraints come from (i) $\Delta F = 1$ processes dominated by tree-level charged current interactions, and (ii) $\Delta F = 2$ meson mixing processes, which only arise at loop level. Therefore, it is simple to modify the CKM fit to constrain new physics in $\Delta F = 2$ processes, under the assumption that it does not significantly affect the SM tree-level charged-current interactions [2]. Within this framework (for a review, see [3]), we can parameterize the NP contributions to the $B_{d,s}$ mixing amplitudes as

$$M_{12}^{d,s} = (M_{12}^{d,s})_{\rm SM} \times \left(1 + h_{d,s}\, e^{2i\sigma_{d,s}}\right). \qquad (1)$$

Until the first measurements of α and γ around 2003, it was not known if the SM gives the leading contribution to $B_d - \overline{B}_d$ mixing [4, 5] (similarly, for $B_s - \overline{B}_s$ mixing, the LHCb constraint on $\sin 2\beta_s$ was needed).

The motivation for the above parameterization is that any NP contribution to M_{12} is additive, and using Eq. (1) one can easily read off both the magnitude and the CP violating phase of the total NP contribution. In particular, for a NP contribution to the mixing of a meson with

	2003	2013	Stage I		Stage II	
$\lvert V_{ud}\rvert$	0.9738 ± 0.0004	$0.97425 \pm 0 \pm 0.00022$	id		id	
$\lvert V_{us}\rvert$ $(K_{\ell 3})$	$0.2228 \pm 0.0039 \pm 0.0018$	$0.2258 \pm 0.0008 \pm 0.0012$	0.22494 ± 0.0006		id	
$\lvert\epsilon_K\rvert$	$(2.282 \pm 0.017) \times 10^{-3}$	$(2.228 \pm 0.011) \times 10^{-3}$	id		id	
Δm_d [ps^{-1}]	0.502 ± 0.006	0.507 ± 0.004	id		id	
Δm_s [ps^{-1}]	> 14.5 [95% CL]	17.768 ± 0.024	id		id	
$\lvert V_{cb}\rvert \times 10^3$ $(b \to c\ell\bar{\nu})$	$41.6 \pm 0.58 \pm 0.8$	$41.15 \pm 0.33 \pm 0.59$	42.3 ± 0.4	[17]	42.3 ± 0.3	[17]
$\lvert V_{ub}\rvert \times 10^3$ $(b \to u\ell\bar{\nu})$	$3.90 \pm 0.08 \pm 0.68$	$3.75 \pm 0.14 \pm 0.26$	3.56 ± 0.10	[17]	3.56 ± 0.08	[17]
$\sin 2\beta$	0.726 ± 0.037	0.679 ± 0.020	0.679 ± 0.016	[17]	0.679 ± 0.008	[17]
α (mod π)	—	$(85.4^{+4.0}_{-3.8})^\circ$	$(91.5 \pm 2)^\circ$	[17]	$(91.5 \pm 1)^\circ$	[17]
γ (mod π)	—	$(68.0^{+8.0}_{-8.5})^\circ$	$(67.1 \pm 4)^\circ$	[17, 18]	$(67.1 \pm 1)^\circ$	[17, 18]
β_s	—	$0.0065^{+0.0450}_{-0.0415}$	0.0178 ± 0.012	[18]	0.0178 ± 0.004	[18]
$\mathcal{B}(B \to \tau\nu) \times 10^4$	—	1.15 ± 0.23	0.83 ± 0.10	[17]	0.83 ± 0.05	[17]
$\mathcal{B}(B \to \mu\nu) \times 10^7$	—	—	3.7 ± 0.9	[17]	3.7 ± 0.2	[17]
$A^d_{\rm SL} \times 10^4$	10 ± 140	23 ± 26	-7 ± 15	[17]	-7 ± 10	[17]
$A^s_{\rm SL} \times 10^4$	—	-22 ± 52	0.3 ± 6.0	[18]	0.3 ± 2.0	[18]
$\bar{m}_c$	$1.2 \pm 0 \pm 0.2$	$1.286 \pm 0.013 \pm 0.040$	1.286 ± 0.020		1.286 ± 0.010	
$\bar{m}_t$	167.0 ± 5.0	$165.8 \pm 0.54 \pm 0.72$	id		id	
$\alpha_s(m_Z)$	$0.1172 \pm 0 \pm 0.0020$	$0.1184 \pm 0 \pm 0.0007$	id		id	
B_K	$0.86 \pm 0.06 \pm 0.14$	$0.7615 \pm 0.0026 \pm 0.0137$	0.774 ± 0.007	[19, 20]	0.774 ± 0.004	[19, 20]
f_{B_s} [GeV]	$0.217 \pm 0.012 \pm 0.011$	$0.2256 \pm 0.0012 \pm 0.0054$	0.232 ± 0.002	[19, 20]	0.232 ± 0.001	[19, 20]
B_{B_s}	1.37 ± 0.14	$1.326 \pm 0.016 \pm 0.040$	1.214 ± 0.060	[19, 20]	1.214 ± 0.010	[19, 20]
f_{B_s}/f_{B_d}	$1.21 \pm 0.05 \pm 0.01$	$1.198 \pm 0.008 \pm 0.025$	1.205 ± 0.010	[19, 20]	1.205 ± 0.005	[19, 20]
B_{B_s}/B_{B_d}	1.00 ± 0.02	$1.036 \pm 0.013 \pm 0.023$	1.055 ± 0.010	[19, 20]	1.055 ± 0.005	[19, 20]
$\tilde{B}_{B_s}/\tilde{B}_{B_d}$	—	$1.01 \pm 0 \pm 0.03$	1.03 ± 0.02		id	
$\tilde{B}_{B_s}$	—	$0.91 \pm 0.03 \pm 0.12$	0.87 ± 0.06		id	

TABLE I. Central values and uncertainties used in our analysis (see definitions in Ref. [10]). The entries "id" refer to the value in the same row in the previous column. The 2003 and 2013 values correspond to Lepton-Photon 2003 and FPCP 2013 conferences [4]. The assumptions entering the Stage I and Stage II estimates are described in the text.

$q_i\bar{q}_j$ flavor quantum numbers due to the operator

$$\frac{C_{ij}^2}{\Lambda^2}\,(\bar{q}_{i,L}\gamma^\mu q_{j,L})^2\,, \tag{2}$$

one finds that

$$h \simeq 1.5\,\frac{|C_{ij}|^2}{|\lambda^t_{ij}|^2}\,\frac{(4\pi)^2}{G_F\Lambda^2} \simeq \frac{|C_{ij}|^2}{|\lambda^t_{ij}|^2}\left(\frac{4.5\,\text{TeV}}{\Lambda}\right)^2,$$
$$\sigma = \arg\big(C_{ij}\,\lambda^{t*}_{ij}\big), \tag{3}$$

where $\lambda^t_{ij} = V^*_{ti}\,V_{tj}$ and V is the CKM matrix. We used NLO expressions for the SM and LO for NP, and neglected running for NP above the top mass. Operators of different chiralities have conversion factors differing by $\mathcal{O}(1)$ factors [6]. Minimal flavor violation (MFV), where the NP contributions are aligned with the SM ones, correspond to $\sigma = 0$ (mod $\pi/2$).

Analogously, in K mixing, we choose to parameterize NP via an additive term to the so-called tt contribution to M_{12}^K in the SM. This is justified by the short distance nature of NP, by the fact that in many NP models the largest contribution to M_{12}^K arise mostly via effects involving the third generation ("23–31" mixing), and more practically, since this allows one to maintain a consistent normalization for NP across the three down-type neutral meson systems. In this paper, D-meson mixing is not considered, due to the large uncertainties related to long-distance contributions.

Comments are in order concerning our assumption of neglecting NP in charged current $b \to u, c$ transitions. If a NP contamination is present and has a different chiral structure than the SM, it will manifest itself by modifying decay distributions, such as the lepton spectrum in semileptonic B decays. On the contrary, if NP has the same chiral structure as the SM, it cannot be physically separated in the determination of $\bar{\rho}$ and $\bar{\eta}$. In such a case, the extracted values of these parameters will not correspond to their SM values. This discrepancy will propagate to the NP fit, and will manifest itself as a nonzero value for $h_{d,s}$ [7], with a specific pattern for $h_{d,s}$ and $\sigma_{d,s}$.

III. GENERIC FIT FOR B_d AND B_s MIXINGS

Table I shows all inputs and their uncertainties used in our fit, performed using the CKMfitter package [4, 8, 9] with its extension to NP in $\Delta F = 2$ [10] (for other studies of such NP, see Refs. [5, 11–16]). We use standard SM notation for the inputs, even for quantities affected by NP in $\Delta F = 2$ whose measurements should be reinterpreted to include NP contributions (e.g. α, β, β_s). We consider 2003 (before the first measurements of α and γ) and 2013 (as of the FPCP 2013 conference), and two future epochs, keeping in mind that any estimate of future progress involves uncertainties on both experimen-

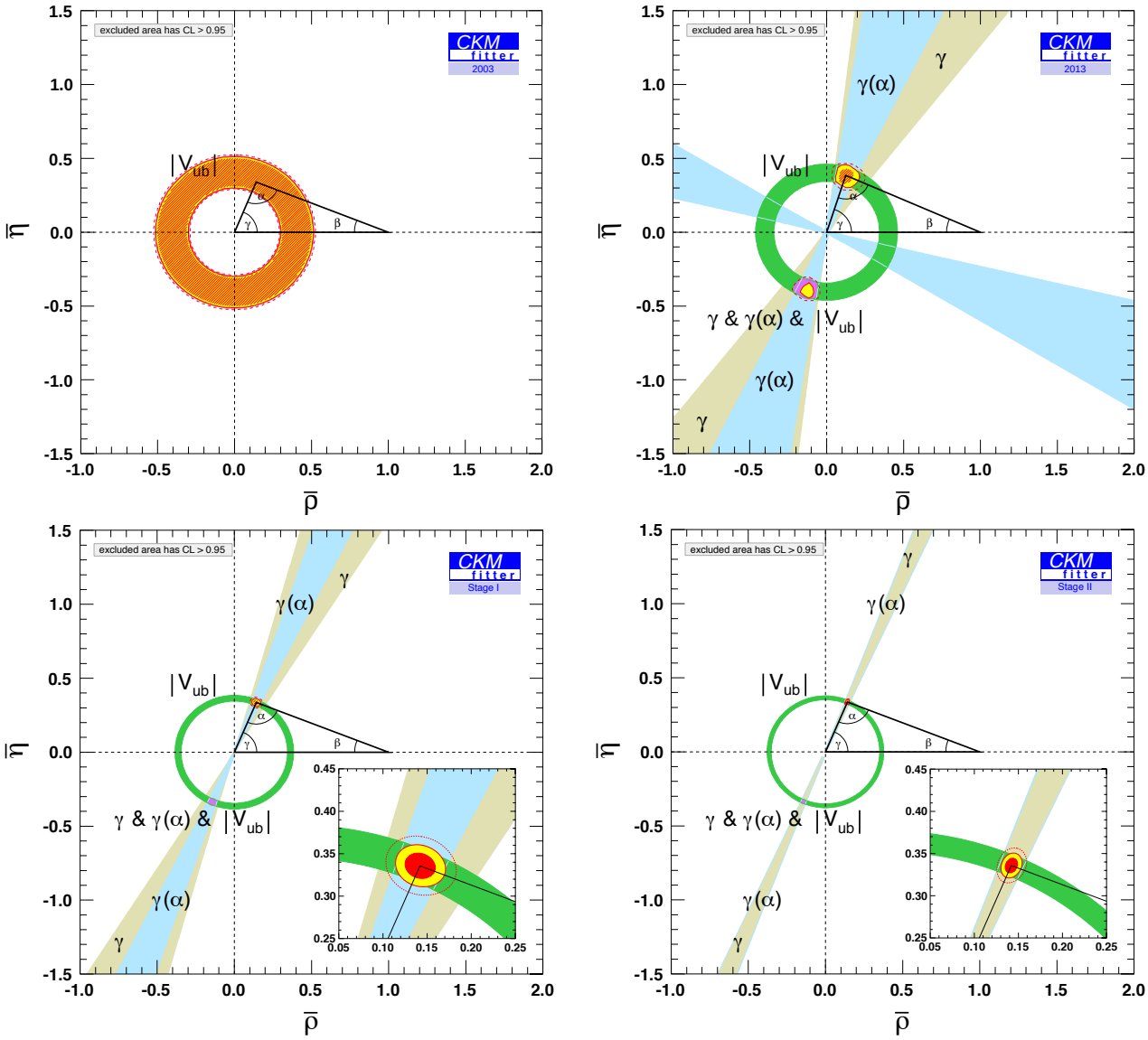

FIG. 1. The past (2003, top left) and present (top right) status of the unitarity triangle in the presence of NP in neutral-meson mixing. The lower plots show future sensitivities for Stage I and Stage II described in the text, assuming data consistent with the SM. The combination of all constraints in Table I yields the red-hatched regions, yellow regions, and dashed red contours at 68.3% CL, 95.5% CL, and 99.7% CL, respectively.

tal and theoretical sides. Our Stage I projection refers to a time around or soon after the end of LHCb Phase I, corresponding to an anticipated $7\,\mathrm{fb}^{-1}$ LHCb data and $5\,\mathrm{ab}^{-1}$ Belle II data, towards the end of this decade. The Stage II projection assumes $50\,\mathrm{fb}^{-1}$ LHCb and $50\,\mathrm{ab}^{-1}$ Belle II data, and probably corresponds to the middle of the 2020s, at the earliest. Estimates of future experimental uncertainties are taken from Refs. [17, 18, 21, 22]. (Note that we display the units as given in the LHCb and Belle II projections, even if it makes some comparisons less straightforward; e.g., the uncertainties of both β and β_s will be $\sim 0.2^\circ$ by Stage II.) For the entries in Table I where two uncertainties are given, the first one is statistical (treated as Gaussian) and the second one is systematic (treated through the Rfit model [8]). Considering the difficulty to ascertain the breakdown between statistical and systematic uncertainties in lattice QCD inputs for the future projections, for simplicity, we treat all such future uncertainties as Gaussian.

The fits include the constraints from the measurements of $A_{\mathrm{SL}}^{d,s}$ [10, 11], but not their linear combination [23], nor from $\Delta\Gamma_s$, whose effects on the future constraints on NP studied in this paper are small. While $\Delta\Gamma_s$ is in agreement with the CKM fit [10], there are tensions for A_{SL} [23]. The large values of h_s allowed until recently, corresponding to $(M_{12}^s)_{\mathrm{NP}} \sim -2(M_{12}^s)_{\mathrm{SM}}$, are excluded by the LHCb measurement of the sign of $\Delta\Gamma_s$ [24]. We do not consider K mixing for the fits shown in this Section,

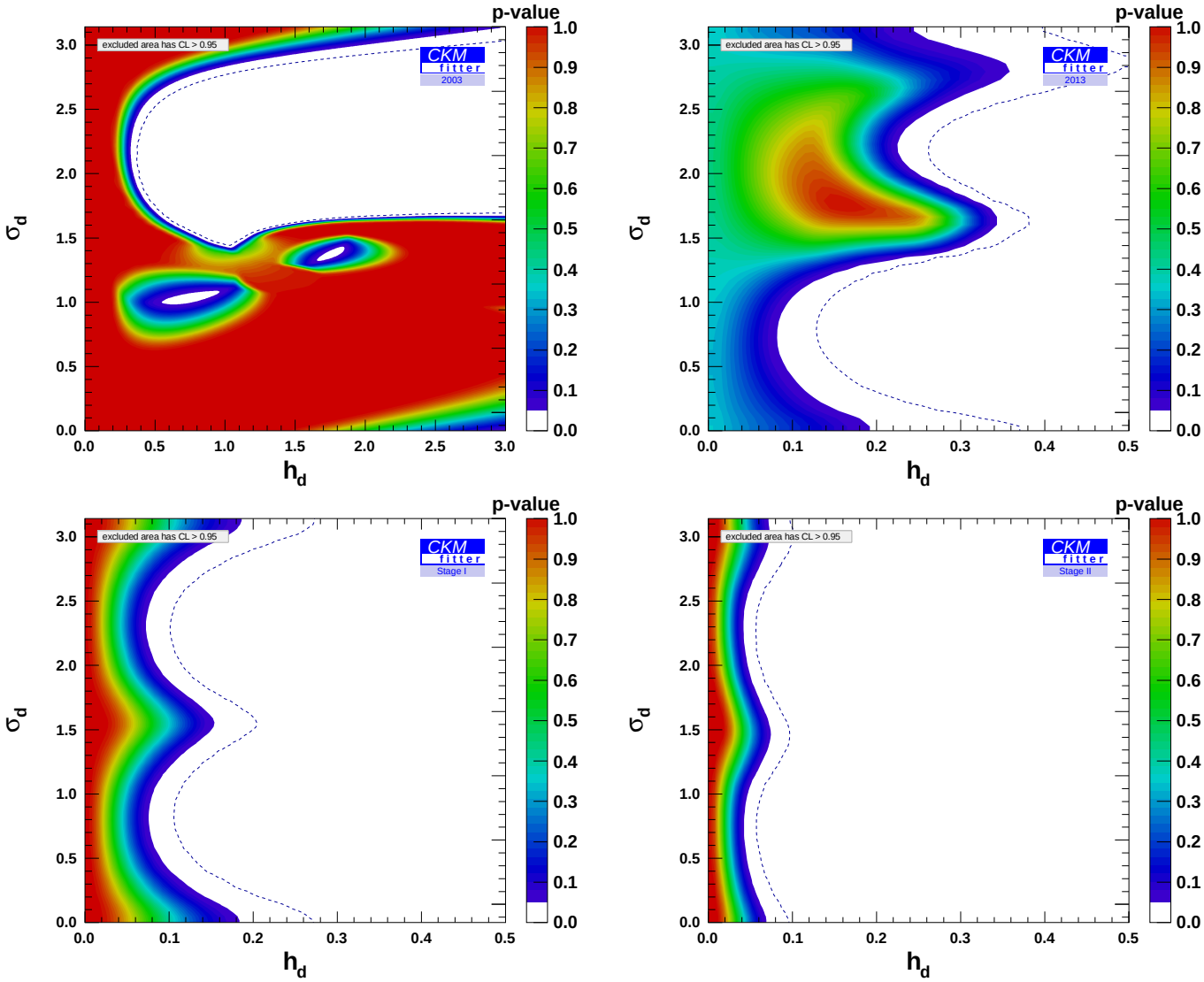

FIG. 2. The past (2003, top left) and present (top right) constraints on $h_d - \sigma_d$ in B_d mixing. The lower plots show future sensitivities for Stage I and Stage II described in the text, assuming measurements consistent with the SM. The dotted curves show the 99.7% CL contours.

as it may receive NP contributions unrelated to B_d and B_s mixings in the general case considered in this section.

Figure 1 shows the evolution of the constraints on $(\bar{\rho}, \bar{\eta})$ in the presence of NP in both B_d and B_s meson mixings, for 2003, 2013, Stage I, and Stage II.[1] The main constraints on $\bar{\rho}$ and $\bar{\eta}$ come from the tree-level inputs γ and $|V_{ub}|$, and also from the combination $\gamma(\alpha) = \pi - \beta - \alpha$ which is not affected by NP in $\Delta F = 2$ [2]. This constraint is more precise than γ itself until Stage I, but of similar precision by Stage II. The γ and $\gamma(\alpha)$ measurement constraints are known modulo π, leading to a sign ambiguity in the determination of $\bar{\rho}$ and $\bar{\eta}$.[2] The intersection of the γ, $\gamma(\alpha)$ and $|V_{ub}|$ constraints yields two 95.5% CL regions in Fig. 1 (yellow for positive $\bar{\rho}$ and $\bar{\eta}$, mauve for negative $\bar{\rho}$ and $\bar{\eta}$) symmetric with respect to the origin. This degeneracy is lifted by the addition of the other experimental inputs, in particular $A^d_{\rm SL}$, leading to a single and small 95.5% CL region (in yellow) for $\bar{\rho}$ and $\bar{\eta}$. (In 2013, the degeneracy is only partially lifted:

[1] Considering anticipated results from only one experiment, plots similar to Fig. 1, and with a different parameterization, Fig. 2, appear in Refs. [17, 22].

[2] In 2013, the combined constraint from the $\pi\pi$, $\pi\rho$ and $\rho\rho$ data allows a second solution for α near 0, with a lower significance than the SM solution in Table I [4]. This second solution is shown as the negative-slope $\gamma(\alpha)$ wedge in Fig. 1, and is ruled out once combined with the γ constraint. We assume that this low-significance solution will disappear with more data by Stage I.

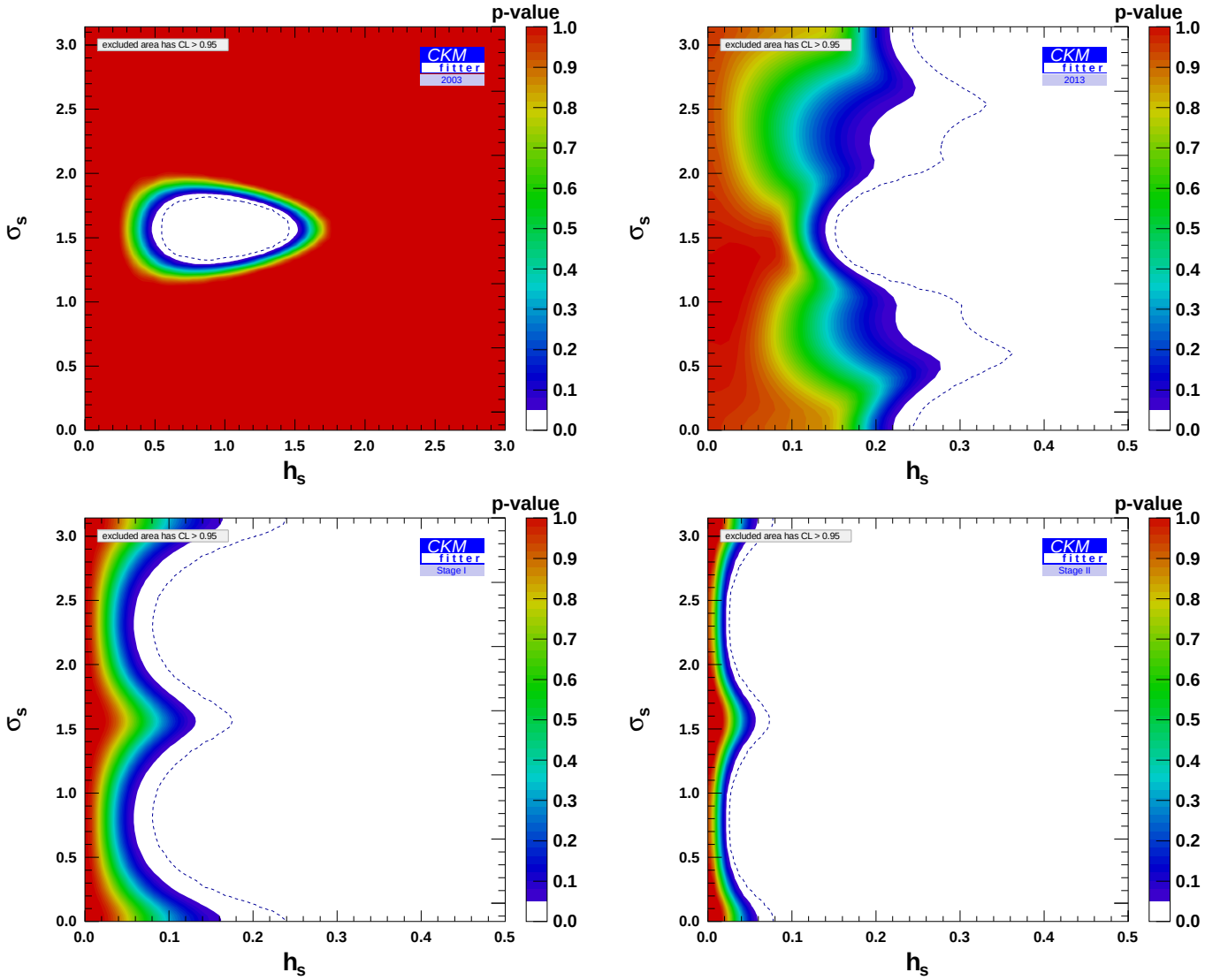

FIG. 3. The past (2003, top left) and present (top right) constraints on $h_s - \sigma_s$ in B_s mixing. The lower plots show future sensitivities for the Stage I and Stage II described in the text, assuming measurements consistent with the SM. The dotted curves show the 99.7% CL contours.

the $\bar{\rho} < 0$, $\bar{\eta} < 0$ solution is excluded at 68.2% CL, but it is allowed at 95.5% CL.)

Figures 2 and 3 show the corresponding evolutions of the constraints on (h, σ) in the B_d and B_s meson systems. Each plot is obtained by considering all the inputs in Table I and treating $\bar{\rho}$, $\bar{\eta}$, and the other physics parameters not shown as nuisance parameters. This corresponds to the case of generic NP, ignoring possible correlations between different $\Delta F = 2$ transitions. Since we are interested in the future sensitivity of LHCb and Belle II to NP, for Stage I and Stage II, we chose the central values of future measurements to coincide with their SM predictions using the current best-fit values of $\bar{\rho}$ and $\bar{\eta}$. Thus, the future best fit corresponds to $h = 0$. Figure 4 shows the projection on the (h_d, h_s) plane.

Future lattice QCD uncertainties for Stage I are taken from Refs. [19, 20] (where they are given as expectations by 2018). These predicted lattice QCD improvements will be very important, mainly for the determination of $|V_{ub}|$ and for the mixing matrix elements, $\langle B_q|(\bar{b}_L\gamma_\mu q_L)^2|\overline{B}_q\rangle = (2/3)\, m_{B_q}^2 f_{B_q}^2 B_{B_q}$. The current expectation is that the uncertainties of f_{B_q} will get below 1%, and may be significantly smaller than those of B_{B_q}. The reduction of the uncertainty of the latter to a similar level would be important. Up to now, due to the chiral extrapolations to light quark masses, more accurate results were obtained for matrix elements involving the B_s meson or for ratios between B_d and B_s hadronic inputs, compared to the results for B_d matrix elements. This leads us to use the former quantities as our lattice inputs for decay constants and bag parameters in Table I. This choice might not be the most suitable one

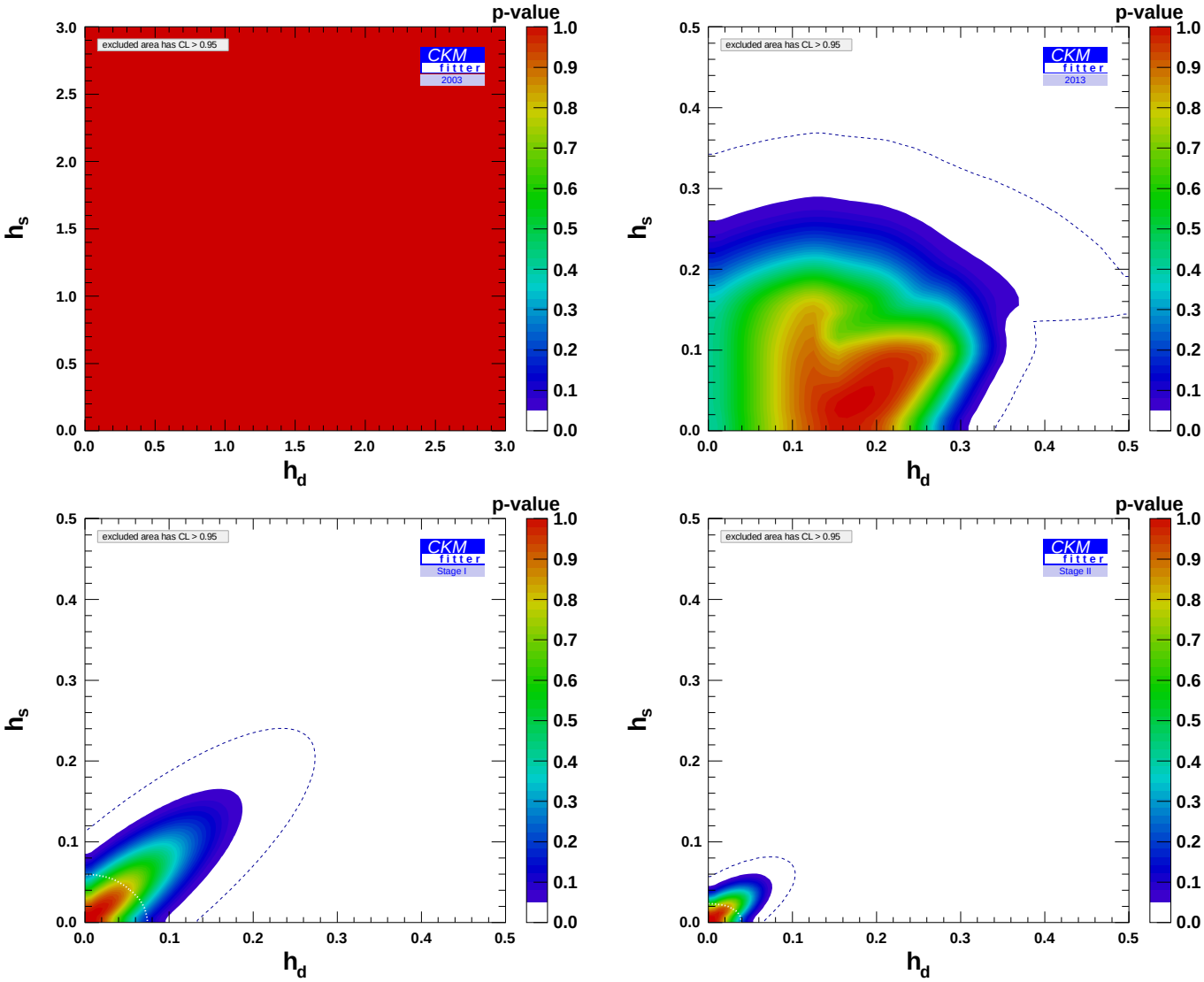

FIG. 4. The past (2003, top left) and present (top right) constraints on $h_d - h_s$ in B_d and B_s mixings. The lower plots show future sensitivities for the Stage I and Stage II scenarios described in the text, assuming measurements consistent with the SM. The dotted curves show the 99.7% CL contours. For Stage I and Stage II, the white dashed curves indicate the 95% CL contours obtained by setting theoretical uncertainties to zero.

in the future, due to improvements in lattice results for light quarks. Concerning $|V_{ub}|$, it is reassuring that 2–3% uncertainty should be obtainable from several measurements: $B \to \tau\nu$, $B \to \mu\nu$, and $B \to \pi\ell\nu$ semileptonic decay. For Stage II, we assumed some additional modest improvements in the lattice QCD inputs, which are important mainly to constrain the MFV-like regions, $\sigma = 0$ mod $\pi/2$. We studied the relative roles of the experimental measurements and the lattice inputs at Stage I and Stage II. In Fig. 4 the white dashed curves indicate the 95% CL contours obtained by setting the theoretical uncertainties to zero, showing no correlation between h_d and h_s. This is different from a realistic situation (including theoretical uncertainties), in which case the correlation between h_d and h_s in the Stage I and II projections in Fig. 4 is driven by our current choice of ratios of B_d and B_s hadronic matrix elements as lattice inputs. This may not reflect the way lattice results will improve in the future, and correlations will affect the shape of the allowed regions in those plots.

From the discussion in the introduction, one may think that $\bar{\rho}$ and $\bar{\eta}$ are determined mostly by SM tree-level processes ($|V_{ub}/V_{cb}|$ and γ from $B \to DK$ decays), while the additional loop-level observables in the standard CKM fit constrain the NP. In particular, $\Delta M_{d,s}$, $\sin 2\beta_{d,s}$, and α would constrain $h_{d,s}$ and $\sigma_{d,s}$, while ϵ_K constrains h_K and σ_K. This simple separation of SM and NP has not been possible yet, given the large uncertainty of γ compared to the combination, $\gamma(\alpha) \equiv \pi - \beta - \alpha$, which is independent of NP in the classes of models under con-

sideration [2]. (Note that in the determination of α from $B \to \rho\rho$, $\rho\pi$, $\pi\pi$, an isospin analysis is used to remove the penguin contribution. To use this measurement to constrain new physics in mixing, one has to assume that NP conserves isospin, which holds in most scenarios, and is strongly supported by data.) As one can clearly see from Table I and Fig. 1, when the direct measurement of γ becomes as precise as $\pi - \beta - \alpha$ in the future, the separation of the two sectors will be simpler to understand, even in a combined SM + NP fit.

For our analysis, precise determination of CKM parameters from tree-level measurements is essential, as illustrated in Fig. 1. Depending on future experimental results, the tension between inclusive and exclusive $|V_{ub}|$ (and $|V_{cb}|$) determinations might remain a cause for concern [25]. The CKM part of our analysis also relies on the expectation that the determination of γ will indeed reach the 1° level. (For α, a comparison of the $\rho\rho$, $\pi\pi$, $\rho\pi$ results may help to constrain the effects of isospin breaking and to reach the expected accuracy.)

One can see from Figs. 2 and 3 that recent LHCb measurements have imposed comparable constraints on NP in B_s mixing to those in the B_d system. This qualitative picture will continue to hold for Stage I and Stage II. At Stage I, we will have $h_{d,s} \lesssim 0.1$ for generic NP phases, with an improvement by an additional factor of more than two at Stage II. This is not surprising, as the uncertainties on β and β_s will be comparable, and improvements in the determination of $\bar\rho$ and $\bar\eta$ from γ and $|V_{ub}/V_{cb}|$ will affect the constraints on the two systems in a similar way. It is also interesting to see that the MFV regions ($\sigma_{d,s} = 0 \bmod \pi/2$) will be less constrained also in the future. Figure 4 provides a different view of these results, by showing the magnitudes of NP allowed in the B_d vs. B_s systems.

The better than factor-of-four improvement in the sensitivity to $h_{d,s}$ from the current constraints to Stage II, more than doubles the energy range probed by these observables, and parallels the improvements in the high energy reach of the LHC, going from LHC7 to LHC14. If NP contains the same CKM suppressions of $\Delta F = 2$ transitions as those present for the SM contributions, typical for models with nontrivial flavor structure in the LHC energy range, the scales probed by the mixing constraints are

$$\Lambda \sim 17\,\text{TeV} \quad (B_d)\,, \qquad \Lambda \sim 19\,\text{TeV} \quad (B_s)\,. \tag{4}$$

Here we used Eq. (3) with $|C_{ij}| = |\lambda^t_{ij}|$, and the 95% CL bounds, $h_d < 0.07$ and $h_s < 0.06$ from Figs. 2 and 3. If, instead, we use $|C_{ij}| = 1$ (corresponding to non-hierarchical NP contributions), the probed scales are

$$\Lambda \sim 2\times 10^3\,\text{TeV} \quad (B_d)\,, \qquad \Lambda \sim 5\times 10^2\,\text{TeV} \quad (B_s)\,. \tag{5}$$

Equation (4) implies that LHCb and Belle II will probe new particles with CKM-like couplings with masses, M, in the 10–20 TeV range if they contribute at tree level (i.e., $\Lambda \sim M$), and in the 1–2 TeV range if they enter with a loop suppression (i.e., $\Lambda \sim 4\pi M$). Considering color factors, RGE effects, etc., which can differ for other operators, one sees that these constraints are in the ballpark of gluino masses explored at LHC14 [26].

IV. INCLUDING NEW PHYSICS IN K MIXING

Next, we consider the neutral kaon system, in addition to B_d and B_s. We only include the constraint from ϵ_K, since there are large uncertainties in the long-distance contribution to Δm_K (for the same reason, we do not study D-meson mixing). Figure 5 shows the evolution of the constraints on NP in K mixing. Larger values of h_K for certain values of the CP-violating phase will still be allowed, even at Stage II. Due to the presence of only one observable, ϵ_K, constraining two parameters, h_K and σ_K, such "throats" cannot be eliminated. They correspond to the values for which the imaginary part of the NP contribution vanishes, that is $\sigma_K \sim \pi - \beta^{\rm SM}$ or $\pi/2 - \beta^{\rm SM}$, where $\beta^{\rm SM}$ is the value of the true CKM β angle shown in Figure 1. In the 2013 plot, the two additional branches with low p-values correspond to the less favored second solution for the CKM parameters $\bar\rho < 0$, $\bar\eta < 0$.

NP contributions as large as 30% of the SM tt contribution will be allowed in the future, even in the MFV case, as can be seen by considering the $\sigma_K = 0, \pi/2$ values in the Stage II plot in Fig. 5. Note that the improvement from Stage I to Stage II is much less significant than the one from the current status to Stage I. Indeed, despite the almost factor-of-two improvement on the uncertainty on B_K and the improvements on $\bar\rho$ and $\bar\eta$, other parameters entering ϵ_K are not expected to have similar improvements, as shown in Table I. This includes the uncertainty associated with higher-order terms in the OPE emphasized in Ref. [27], and higher-order QCD corrections discussed in Refs. [28, 29] (in particular for the cc contribution).

In many scenarios with TeV-scale NP, the constraints from kaon mixing provide the strongest constraints to date, especially for the case of chirality-flipping left-right (LR) operators, due to chiral enhancements in the matrix elements and stronger QCD running. This situation will be maintained in the Stage II era as well, with comparable constraining power for non-LR NP, and a significant advantage of the kaon system over the $B_{d,s}$ systems in constraining chirality-flipping operators. Furthermore, if NP is decoupled from the weak scale and carries unsuppressed flavor violation (e.g., intermediate-scale split supersymmetric scenarios [30]), the kaon system will provide the most stringent probe (or the first place where a deviation can be observed), since it carries the strongest CKM suppression in the SM.

We next consider more specific NP scenarios, where the contributions to the different neutral-meson systems are correlated. In the MFV case mentioned in Sec. II,

$$h_d = h_s = h_K\,, \qquad 0 = \sigma_d = \sigma_s = \sigma_K \ (\bmod \pi/2)\,. \tag{6}$$

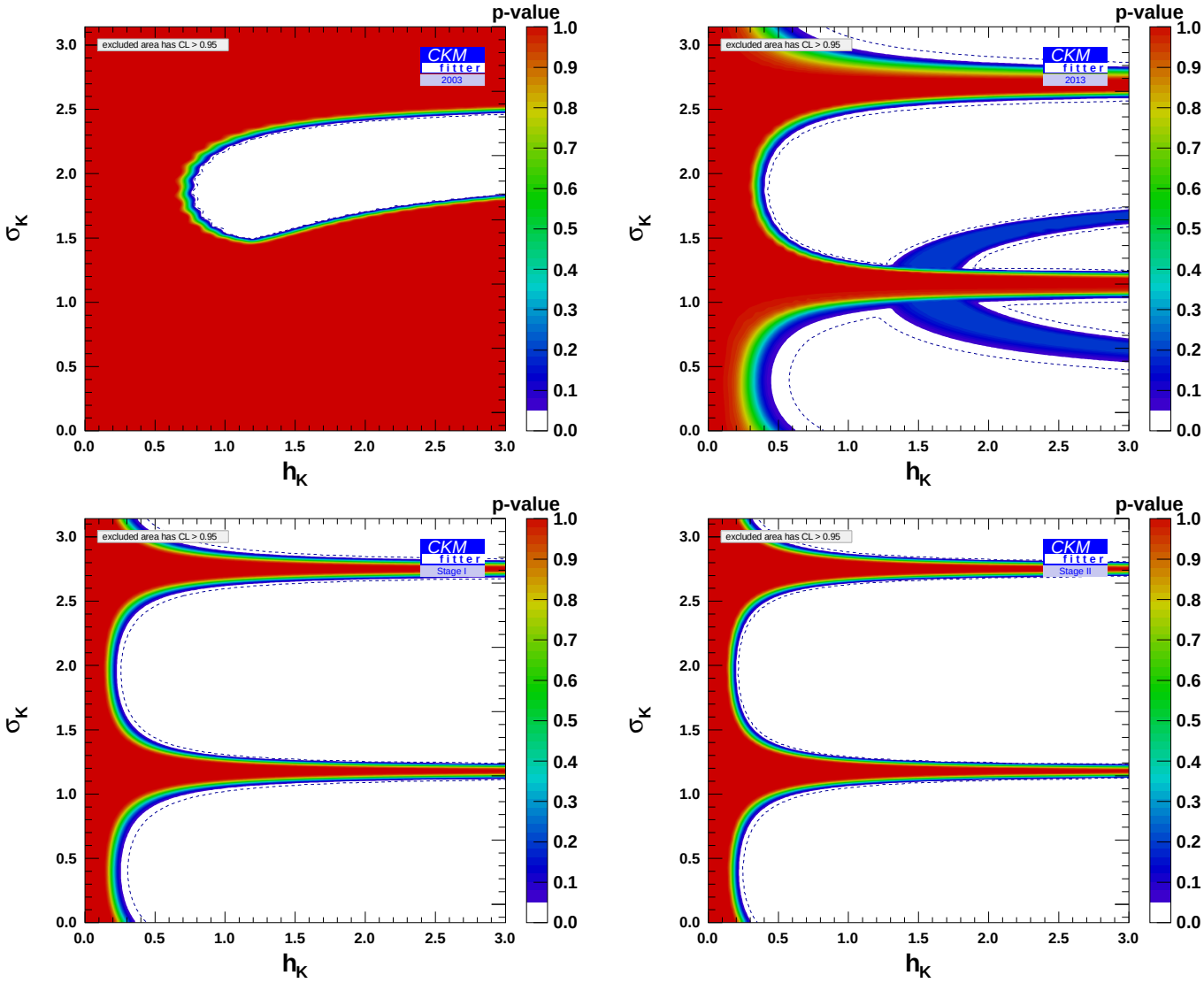

FIG. 5. The past (2003, top left) and present (top right) constraints on $h_K - \sigma_K$ in K mixing. The lower plots show future sensitivities for the Stage I and Stage II scenarios described in the text, assuming measurements consistent with the SM. The dotted curves show the 99.7% CL contours.

Figure 6 shows the p-values for the real (positive or negative) $h \equiv h_d \exp(2i\sigma_d)$ in 2003, 2013, Stage I, and Stage II.

Additional particularly interesting scenarios are those in which the dominant effects are mediated by the third generation, motivated by the natural stabilization of the electroweak scale, and those in which the approximate horizontal $U(2)^3$ symmetry of the SM, induced by $m_{u,c}/m_t \ll 1$ and $m_{d,s}/m_b \ll 1$, also applies to the NP contributions [31, 32]. In the first case, the NP contribution to kaon mixing is attained via mixing with the third generation, and is therefore related to those in B_d and B_s mixings. In a fundamental theory representing this scenario the mixing parameters C_{ij} in the kaon sector, similar to Eq. (2), will be the product of those entering the B_d- and B_s-mixing expressions, up to small corrections. Therefore, there is a correlation among the phases,

$$\sigma_K = \sigma_d - \sigma_s \,. \tag{7}$$

On the other hand, the magnitudes of the NP contributions, $h_{K,d,s}$ also depend on the typical mass scale, coupling constants, and kinematic function, represented by Λ in Eq. (2). Thus, in general, 3rd generation mediation in the kaon system does not imply a relation between h_K and $h_{d,s}$. The constraint on such models is shown in Fig. 7, for the future Stage II scenario. Mild correlations between the limits on the magnitudes of NP in $B_{d,s}$ and K mixings arise due to the relations on the CP phases σ_i described above, and to a lesser extent via $\bar{\rho}$ and $\bar{\eta}$. The plot is easily understood: the largest NP contribution in $B_{d,s}$ mixing is allowed for $\sigma_{d,s} \sim 0$ (mod $\pi/2$), which is allowed for sufficiently small $h_K \lesssim 0.6$. The presence of

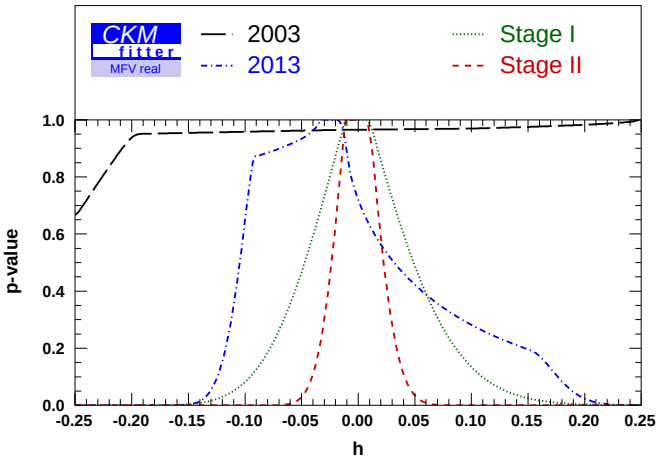

FIG. 6. Constraints on $h \equiv h_d\, e^{2i\sigma_d} = h_s\, e^{2i\sigma_s} = h_K\, e^{2i\sigma_K}$ in MFV scenarios, in which $\sigma_d = \sigma_s = \sigma_K = 0 \pmod{\pi/2}$, for the different epochs considered.

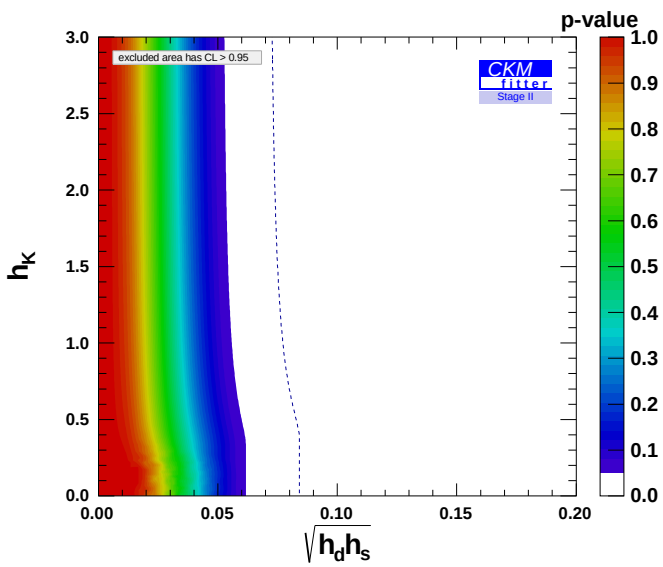

FIG. 7. Correlations between limits on NP in K, B_d and B_s mixing, at "Stage II", in classes of models where flavor violation in K mixing proceeds dominantly via the third generation: $\sigma_K = \sigma_d - \sigma_s$, while $h_{K,d,s}$ are kept free. The dotted curve shows the 99.7% CL contour.

the "throats" in Fig. 5 allow larger values for h_K for the non-$U(2)^3$ case, but at the price of not allowing $\sigma_{s,d} \sim 0 \pmod{\pi/2}$, hence the (small) reduction in the allowed magnitude of NP in the $B_{d,s}$ sector. This effect can be more pronounced, if the actual future data agrees less well with the SM, than assumed in this paper.

In the case of the minimal $U(2)^3$ class of models [33], the NP contributions to B_d and B_s should be equal. Furthermore, minimality implies that the bulk of the NP contribution in the kaon sector is controlled by the same spurions as in the $B_{d,s}$ sectors via 3rd generation mediation, "23–31". Therefore, one has

$$h_B \equiv h_d = h_s\,, \qquad \sigma_B \equiv \sigma_d = \sigma_s\,, \qquad \sigma_K = 0\,. \tag{8}$$

The constraints on such scenarios are shown in Figs. 8 and 9. In Fig. 8 the minimal $U(2)^3$ scenario is shown in the $h_B - \sigma_B$ plane. While the 2003 and 2013 fits show interesting patterns arising from the combination of the $B_{d,s}$ constraints, the future projections for the $U(2)^3$ models look very similar to Figs. 2 and 3.

The correlation between the limits on the magnitudes of NP in $B_{d,s}$ and K mixings in the minimal $U(2)^3$ case is shown in Fig. 9 in the h_K–h_B plane. Similar considerations as in Fig. 7 apply here. As can be seen in Fig. 5, the constraint $\sigma_K = 0$ limits the size of $h_K \lesssim 0.25$.

In the case of generic $U(2)^3$ models, which allow additional NP contributions in the kaon system unrelated to those in the $B_{d,s}$ systems, $h_d = h_s$ and $\sigma_d = \sigma_s$ are maintained, but the correlation with the K systems is lost. Therefore, the constraints in Fig. 9 no longer apply, while those in Fig. 8 are still valid.

Constraints on NP in K mixing will improve if lattice QCD gives a precise SM calculation of Δm_K [34]. For $\mathrm{Re}(M_{12}^K)$ in the SM, the ratio of the tt and cc contributions is about 0.5%, so a 1% calculation of Δm_K could exclude $h_K \gtrsim 2$. Lattice QCD progress may also reduce the uncertainty in the higher order terms in ϵ_K discussed in Ref. [27], improving the overall constraints. Due to its unpredictability, we do not include possible improvements in this term (κ_ϵ) in our Stage I and II fits. Even assuming a much reduced uncertainty of η_{cc}, ± 0.2 instead of ± 0.76 at NNLO now (see Ref. [35]), would only improve the bounds on h_K shown in Fig. 5 slightly; e.g., at Stage II for $\sigma_K = 0$, from $h_K < 0.31$ to $h_K < 0.24$.

In certain classes of models, improvement in sensitivity compared to Fig. 5 can also arise from future measurements of $K^+ \to \pi^+\nu\bar{\nu}$ and $K_L \to \pi^0\nu\bar{\nu}$ [36]. These decays are also sensitive to NP in $s \to d$ penguins, which can be parameterized by another magnitude $h_K^{(\Delta S=1)}$ and phase $\sigma_K^{(\Delta S=1)}$; thus the difference of the number of observables vs. NP parameters will not change. However, in certain well-motivated scenarios, $\sigma_K^{(\Delta S=1)} = \sigma_K$ [12], or $h_K^{(\Delta S=1)} \sim 0$, and in such cases including future data on these rare decays will improve the sensitivity to NP.

V. SUMMARY AND OUTLOOK

We studied the anticipated future improvements in the constraints on NP in B_d, B_s, and K mixings. We found that if no NP signal is seen, the bounds on h_d and h_s will improve by about a factor of 5. This corresponds to probing NP at scales more than a factor of two higher than currently (for a fixed set of couplings). Interestingly, compared to the allowed regions to date, we expect the MFV-like regions, $\sigma = 0 \pmod{\pi/2}$, to be nearly as strongly constrained as those with generic NP phase in the future. Our results for the future sensitivity to a NP

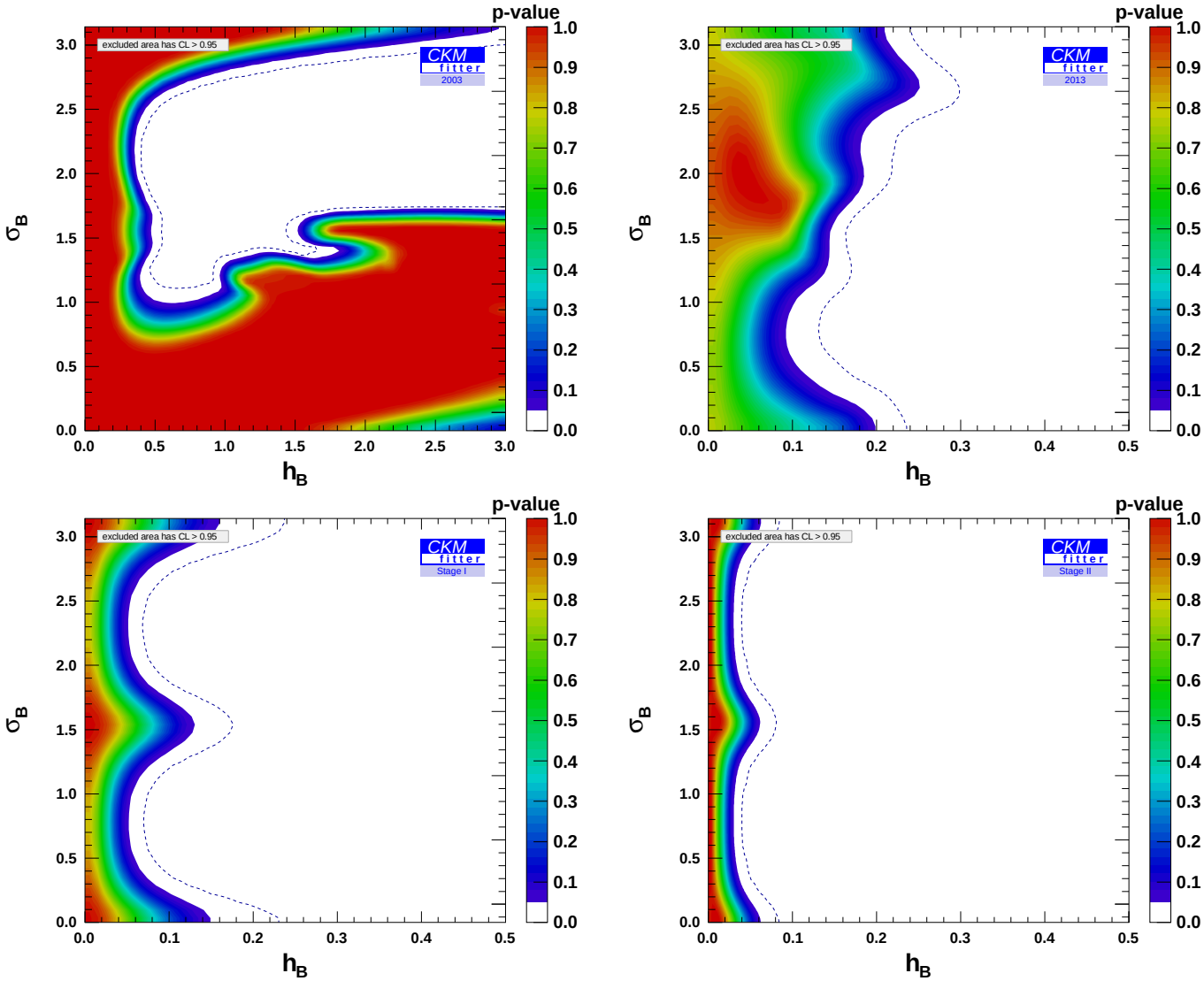

FIG. 8. The past (2003, top left) and present (top right) constraints on $U(2)^3$ scenarios, where $h_B \equiv h_d = h_s$, $\sigma_B \equiv \sigma_d = \sigma_s$. The lower plots show future sensitivities for the Stage I and Stage II scenarios described in the text, assuming measurements consistent with the SM. The dotted curves show the 99.7% CL contours.

contribution given by Eq. (2) in B_d and B_s mixings at Stage II are summarized in Table II. For K mixing, the large h_K regions in Fig. 5 complicate the interpretation in terms of NP scales. If we assume that lattice QCD will exclude $h_K > 2$ as discussed in Sec. IV, we get sensitivity up to 3 TeV (0.3 TeV) at tree level (one loop) for CKM-like couplings, and up to 9×10^3 TeV (7×10^2 TeV) at tree level (one loop) for non-hierarchical couplings.

So far in this paper we assumed that future measurements agree with the SM predictions. However, future data can not only set better bounds on NP, they may also reveal deviations from the SM. This is illustrated in Fig. 10, where we set $\bar{\rho}$, $\bar{\eta}$, $h_{d,s}$ and $\sigma_{d,s}$ to their current best-fit values (allowing for NP in $\Delta F = 2$), and performed a fit assuming for all future measurements the corresponding central values, but uncertainties as given in Table I for Stage II. While any assumption about possible future NP signals includes a high degree of arbitrari-

Couplings	NP loop order	Scales (in TeV) probed by B_d mixing	B_s mixing
$\lvert C_{ij}\rvert = \lvert V_{ti}V_{tj}^*\rvert$	tree level	17	19
(CKM-like)	one loop	1.4	1.5
$\lvert C_{ij}\rvert = 1$	tree level	2×10^3	5×10^2
(no hierarchy)	one loop	2×10^2	40

TABLE II. The scale of the operator in Eq. (2) probed by B_d and B_s mixings at Stage II (if the NP contributions to them are unrelated). The impact of CKM-like hierarchy of couplings and/or loop suppression is indicated.

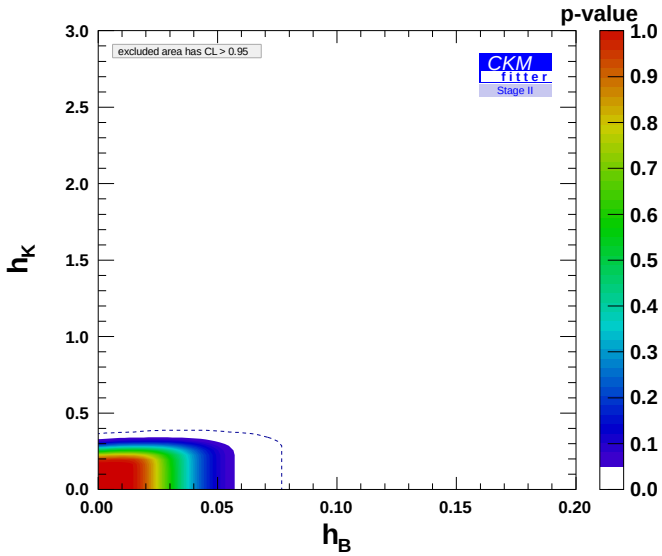

FIG. 9. Correlations between limits on NP in K and $B_{d,s}$ mixing, at "Stage II", in minimal $U(2)^3$ models. This fit corresponds to $h_d = h_s \equiv h_B$, $\sigma_B \equiv \sigma_d = \sigma_s$, and $\sigma_K = 0$. The dotted curve shows the 99.7% CL contour.

ness, Fig. 10 may give an impression of the sensitivity to reveal a deviation from the SM.

Similar predictions could be made for many other higher dimension flavor-changing operators. The $\Delta F = 1$ observables dominated by one-loop contributions in the SM probe different NP contributions. Such analyses have been performed for $b \to s\gamma$, $b \to s\ell^+\ell^-$, etc. [37]. The progress for the constraints imposed by some of these observables, especially those corresponding to not yet observed processes, will be greater than those for B_d and B_s mixings studied in this paper. This example is particularly interesting, as many NP models do predict an effect which may be observable in the coming decade. Furthermore, $\Delta F = 2$ generically provides the strongest constraints for high-scale models with unsuppressed flavor violation, while still providing competitive constraints for lower scale NP (where flavor transitions are parametrically suppressed as in the SM). Finally, the significant improvements on the bounds in the $h - \sigma$ planes for B_d and B_s mixings give an impressive yet conservative illustration of the anticipated future progress coming from the LHCb upgrade and the Belle II experiment.

ACKNOWLEDGMENTS

We thank Riccardo Barbieri, Filippo Sala, and Stéphane T'Jampens for helpful comments. ZL and MP were supported in part by the Office of Science, Office of High Energy Physics, of the U.S. Department of Energy under contract DE-AC02-05CH11231. We would like to thank all members of the CKMfitter group for suggestions on various aspects of this article.

[1] M. Kobayashi and T. Maskawa, Prog. Theor. Phys. **49** (1973) 652.
[2] J. M. Soares and L. Wolfenstein, Phys. Rev. D **47** (1993) 1021; T. Goto, N. Kitazawa, Y. Okada and M. Tanaka, Phys. Rev. D **53** (1996) 6662 [hep-ph/9506311]; J. P. Silva and L. Wolfenstein, Phys. Rev. D **55** (1997) 5331 [hep-ph/9610208]; Y. Grossman, Y. Nir and M. P. Worah, Phys. Lett. B **407** (1997) 307 [hep-ph/9704287].
[3] A. Hocker and Z. Ligeti, Ann. Rev. Nucl. Part. Sci. **56** (2006) 501 [hep-ph/0605217].
[4] J. Charles *et al.* [CKMfitter Group], Eur. Phys. J. C **41** (2005) 1 [hep-ph/0406184]; and updates at `http://ckmfitter.in2p3.fr/`.
[5] Z. Ligeti, Int. J. Mod. Phys. A **20** (2005) 5105 [hep-ph/0408267].
[6] A. J. Buras, S. Jager and J. Urban, Nucl. Phys. B **605**, 600 (2001) [hep-ph/0102316].
[7] P. J. Fox, Z. Ligeti, M. Papucci, G. Perez and M. D. Schwartz, Phys. Rev. D **78**, 054008 (2008) [arXiv:0704.1482 [hep-ph]].
[8] A. Hocker, H. Lacker, S. Laplace and F. Le Diberder, Eur. Phys. J. C **21** (2001) 225 [hep-ph/0104062].
[9] J. Charles *et al.*, Phys. Rev. D **84** (2011) 033005 [arXiv:1106.4041 [hep-ph]].
[10] A. Lenz *et al.*, Phys. Rev. D **83**, 036004 (2011) [arXiv:1008.1593 [hep-ph]]; A. Lenz *et al.*, Phys. Rev. D **86**, 033008 (2012) [arXiv:1203.0238 [hep-ph]].
[11] S. Laplace, Z. Ligeti, Y. Nir and G. Perez, Phys. Rev. D **65** (2002) 094040 [hep-ph/0202010].
[12] K. Agashe, M. Papucci, G. Perez and D. Pirjol, hep-ph/0509117.

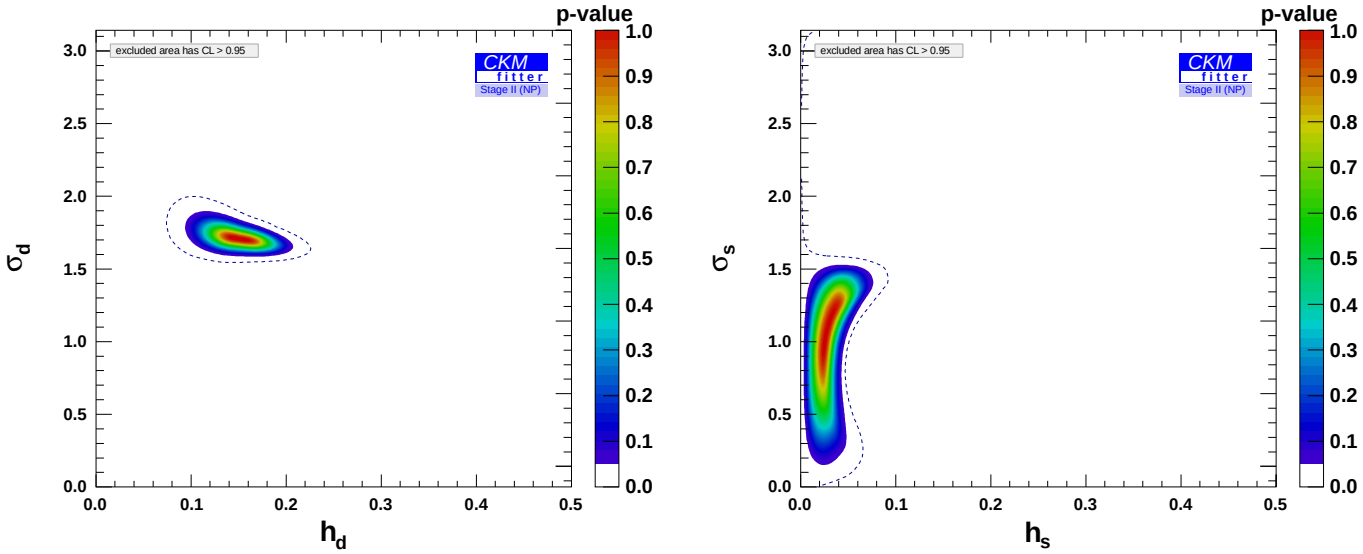

FIG. 10. Hypothetical Stage II fits for NP, assuming that all future experimental results correspond to the current best-fit values of $\bar{\rho}$, $\bar{\eta}$, $h_{d,s}$ and $\sigma_{d,s}$ (with measurement uncertainties as given in Table I, but different central values).

[13] M. Bona *et al.* [UTfit Collaboration], JHEP **0603**, 080 (2006) [hep-ph/0509219]; JHEP **0803**, 049 (2008) [arXiv:0707.0636 [hep-ph]].

[14] Z. Ligeti, M. Papucci and G. Perez, Phys. Rev. Lett. **97** (2006) 101801 [hep-ph/0604112].

[15] G. Isidori, Y. Nir and G. Perez, Ann. Rev. Nucl. Part. Sci. **60** (2010) 355 [arXiv:1002.0900 [hep-ph]].

[16] Z. Ligeti, M. Papucci, G. Perez and J. Zupan, Phys. Rev. Lett. **105** (2010) 131601 [arXiv:1006.0432 [hep-ph]].

[17] T. Aushev *et al.*, arXiv:1002.5012 [hep-ex].

[18] R. Aaij *et al.* [LHCb Collaboration], Eur. Phys. J. C **73** (2013) 2373 [arXiv:1208.3355 [hep-ex]].

[19] T. Blum *et al.*, "Lattice QCD at the Intensity Frontier" `http://www.usqcd.org/documents/13flavor.pdf`.

[20] We thank R. Van De Water for helpful correspondance about future lattice QCD expectations.

[21] B. Meadows *et al.*, arXiv:1109.5028 [hep-ex].

[22] M. Bona *et al.*, arXiv:0709.0451 [hep-ex].

[23] V. M. Abazov *et al.* [D0 Collaboration], Phys. Rev. D **84**, 052007 (2011) [arXiv:1106.6308 [hep-ex]].

[24] R. Aaij *et al.* [LHCb Collaboration], Phys. Rev. Lett. **108**, 241801 (2012) [arXiv:1202.4717 [hep-ex]].

[25] See, e.,g., R. Kowalewski and T. Mannel, "Determination of V_{cb} and V_{ub}"; in J. Beringer *et al.* [Particle Data Group Collaboration], Phys. Rev. D **86** (2012) 010001.

[26] ATLAS Collaboration, arXiv:1307.7292 [hep-ex].

[27] A. J. Buras, D. Guadagnoli and G. Isidori, Phys. Lett. B **688**, 309 (2010) [arXiv:1002.3612 [hep-ph]].

[28] J. Brod and M. Gorbahn, Phys. Rev. D **82** (2010) 094026 [arXiv:1007.0684 [hep-ph]].

[29] J. Brod and M. Gorbahn, Phys. Rev. Lett. **108** (2012) 121801 [arXiv:1108.2036 [hep-ph]].

[30] N. Arkani-Hamed, A. Gupta, D. E. Kaplan, N. Weiner and T. Zorawski, arXiv:1212.6971 [hep-ph].

[31] R. Barbieri, G. Isidori, J. Jones-Perez, P. Lodone and D. M. Straub, Eur. Phys. J. C **71** (2011) 1725 [arXiv:1105.2296 [hep-ph]].

[32] R. Barbieri, D. Buttazzo, F. Sala and D. M. Straub, JHEP **1207**, 181 (2012) [arXiv:1203.4218 [hep-ph]].

[33] R. Barbieri, D. Buttazzo, F. Sala and D. M. Straub, JHEP **1210**, 040 (2012) [arXiv:1206.1327 [hep-ph]].

[34] N. H. Christ, T. Izubuchi, C. T. Sachrajda, A. Soni and J. Yu, arXiv:1212.5931 [hep-lat]; see also S. Sharpe, talk at the ANL Intensity Frontier Workshop, 25–27 April 2013, `https://indico.fnal.gov/getFile.py/access?contribId=126&sessionId=0&resId=0&materialId=slides&confId=6248`, and J. Yu, talk at Lattice 2013, 29 July – 3 August 2013. `http://www.lattice2013.uni-mainz.de/presentations/7C/Yu.pdf`

[35] A. J. Buras and J. Girrbach, arXiv:1304.6835 [hep-ph].

[36] Y. Grossman and Y. Nir, Phys. Lett. B **398**, 163 (1997) [hep-ph/9701313].

[37] T. Hurth *et al.*, Nucl. Phys. B **808** (2009) 326 [arXiv:0807.5039 [hep-ph]]; F. Beaujean *et al.*, JHEP **1208** (2012) 030 [arXiv:1205.1838 [hep-ph]]; S. Descotes-Genon *et al.*, JHEP **1106** (2011) 099 [arXiv:1104.3342 [hep-ph]]; JHEP **1301** (2013) 048 [arXiv:1207.2753 [hep-ph]]; S. Descotes-Genon, J. Matias and J. Virto, arXiv:1307.5683 [hep-ph]; W. Altmannshofer and D. M. Straub, JHEP **1208** (2012) 121 [arXiv:1206.0273 [hep-ph]]; arXiv:1308.1501 [hep-ph].